Reynolds stress and shear flow generation

S. B. Korsholm, P. K. Michelsen, V. Naulin, and J. Juul Rasmussen

Association EURATOM-Risø National Laboratory, OFD-128 Risø, DK-4000 Roskilde

One of the major challenges in the research towards a fusion power plant is the understanding and control of the plasma turbulence leading to anomalous transport of particles and energy.

Experimentally obtained improved scenarios such as H-mode confinement regimes show a drastically reduced radial transport. The generation of H-mode confinement regimes seem to be closely related to poloidal shear flows in the edge region of the plasma. Generally, it is observed experimentally and in numerical models that shear flows in plasmas suppress turbulence and transport. The generation mechanism of these flows is thus of some interest.

As presented analytically in [1] the so-called Reynolds stress gives a measure of the self-consistent flow generation in turbulent fluids and plasmas by the small-scale turbulent fluctuations. A measurement of the Reynolds stress can thus help to predict flows e.g. shear flows in plasmas as demonstrated in [2]. However, the determination of the Reynolds stress requires measurements of the plasma potential which is difficult to measure in general and nearly impossible in large plasma devices.

In this work we investigate an alternative method, which is based on density measurements, to estimate the Reynolds stress, and demonstrate the validity range of this quantity which we term the pseudo-Reynolds stress. The advantage of such a quantity is that accurate measurements of density fluctuations is much easier to obtain. Prior to the treatment of the pseudo-Reynolds stress we present analytical and numerical drift wave turbulence results which demonstrate that the Reynolds stress in a plasma, indeed, generate a poloidal shear flow.

The model used in the numerical investigations was the three dimensional drift wave Hasegawa-Wakatani model [3]. One of the strengths of the model is that fluctuations and background may be evaluated in one instance, i.e. the background and the fluctuations are separated, but the interaction between these is included. The back-reaction of the density fluctuations on the background density gradient, however, is not recoverable from previous Hasegawa-Wakatani simulations, due to use of periodic geometries (See e.g. [4]). Furthermore, the use of a triply periodic geometry may not be valid in many configurations. For the case of the Hasegawa-Wakatani model the final state the system evolves into invalidates some of the underlying assumptions [4]. Therefore, in a slab geometry periodic in y and z (corresponding to the poloidal and toroidal directions respectively) we use non-permeable walls in the radial direction, i.e. Dirichlet boundaries in x ($\phi(x = 0) = \phi(x = L_x) = 0$ and $n(x = 0) = n(x = L_x) = 0$). Thus a back-reaction of the density fluctuations on the background density gradient is possible.

We use the Hasegawa-Wakatani equations with the background density of the form $n_0 = n_0(x) = N_0 e^{-\frac{x}{L_n}}$. The equations in normalised dimensionless variables are thus:

$$(\frac{\partial}{\partial t} + \mathbf{v}_E \cdot \nabla_\perp)n + \frac{\partial \phi}{\partial y} = \mathcal{C}\frac{\partial^2}{\partial z^2}(n - \phi) + \nu\nabla_\perp^2 n \tag{1}$$

$$(\frac{\partial}{\partial t} + \mathbf{v}_E \cdot \nabla_\perp)(\nabla_\perp^2 \phi) = \mathcal{C}\frac{\partial^2}{\partial z^2}(n - \phi) + \nu\nabla_\perp^4 \phi \tag{2}$$

Note that the parallel resistivity has been included in the normalisation of the parallel scales (z), while the ion gyro-radius at electron temperature, $\rho_s = \frac{\sqrt{T_e m_i}}{e B_0}$, has been used to normalise lengths perpendicular to $\mathbf{B}$ (x and y).

The simulations were performed by Fourier spectral methods using only sine transforms in the radial direction, since these obviously are zero at $x = 0$, $x = L_x$. The number of modes in the simulations presented here is 64 in the perpendicular directions (x and y) and 32 in the direction parallel to the magnetic field. The domain size was $L_x = L_y = 30$ and $L_z = 20$ and the time step $dt = 4 \cdot 10^{-3}$. The relatively low number of modes necessitated the use of a high viscosity parameter of $\nu = 0.03$.

The energy of the turbulence in these Dirichlet boundary simulations is significantly reduced compared to periodic boundary simulations. The reason for this observed reduced growth is the back-reaction of the density fluctuations on the background density. The fluctuations organise to flatten the background profile and the effective gradient is flattened. Consequently the drive of the turbulence is quenched. The $\frac{\partial \phi}{\partial y}$-term in equation (1) originate from the background profile, and the back-reaction of the fluctuations on this is through the nonlinear term, where also a $\frac{\partial \phi}{\partial y}$-term occurs.

Another equally valid view is that the turbulence organises into a poloidal shear flow having $k_y = 0$, i.e. the drive from the $\frac{\partial \phi}{\partial y}$-term is quenched. This property of the small-scale plasma turbulence organising into a shear flow can be explained by the theory of Reynolds stress.

The Reynolds stress is a measure of the anisotropy of the turbulent velocity fluctuations, since it is generated solely from inhomogeneous correlations between v_x and v_y. As shown in [5] anisotropic velocity fluctuations produce a stress on the mean flow. This cause an acceleration of the flow in the plasma, which e.g. could be a poloidal flow (y-direction in the slab geometry). A self-consistent explanation of the flow generation is that for drift wave turbulence the Reynolds stress can be seen as a flow of charge due to the nonlinear polarisation drift [6]. This creates a radial electric field which combined with the toroidal magnetic field generates the poloidal flow.

The Reynolds stress is interesting to measure experimentally, since large flows may be predicted [2]. By comparison of Reynolds stresses of different plasma machines it may be possible to say whether a larger flow could be expected. This has an interest, since this poloidal flow may be responsible for the L– to H–mode transition. The Reynolds stress is defined as

$$\text{Re}_\phi = -\langle v_x v_y \rangle = \left\langle \frac{\partial \phi}{\partial y} \frac{\partial \phi}{\partial x} \right\rangle \tag{3}$$

An experimental determination of the Reynolds stress demands an accurate measurement of the fluctuations in the electrostatic potential. This, unfortunately, is quite difficult, especially in large plasma devices [2, 7].

It has therefore been suggested that an approximate value of the Reynolds stress may be obtained from the density perturbations. This density-based pseudo-Reynolds stress is defined as:

$$\text{Re}_n = \left\langle \frac{\partial n}{\partial y} \frac{\partial n}{\partial x} \right\rangle \tag{4}$$

If a correlation exists between Re_n and Re_ϕ it will be sufficient to measure the density fluctuations, which is easier than measurements of the electrostatic potential. Since often

ϕ and n are strongly correlated in the drift wave limit, i.e. for $k_{\parallel} \neq 0$ (See Figure 1), we performed numerical simulations, with the purpose of determining whether a density-based pseudo-Reynolds stress is in fact strongly correlated to the real Reynolds stress. In the edge of experimental plasmas confined by a sheared magnetic field, no modes having $k_{\parallel} = 0$ exist. Hence it is reasonable to exclude the convective cell in the Reynolds stress calculations and only use the drift wave components. The temporal evolution of the spatial correlation (for zero time lag) of the drift components of the Reynolds stress and the pseudo-Reynolds stress $\langle \mathrm{Re}_{\phi(k_{\parallel} \neq 0)} \mathrm{Re}_{n(k_{\parallel} \neq 0)} \rangle_{xyz}$ are presented in Figure 2 and are seen to be reasonably high. By averaging the Hasegawa-Wakatani equation (2) one obtain
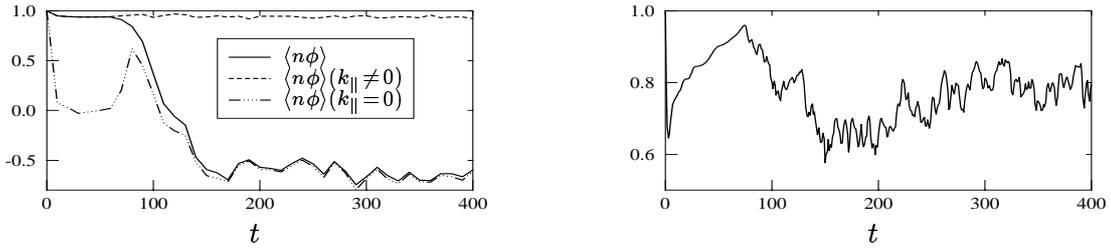

Figure 1: *The temporal evolution of the 3D spatial correlation of n and ϕ for all $k_{\parallel}$, for the drift modes ($k_{\parallel} \neq 0$), and for the convective cell modes ($k_{\parallel} = 0$).*

Figure 2: *The temporal evolution of the spatial correlation of the Reynolds stress and the pseudo-Reynolds stress for the drift components only.*

$$\frac{\partial \langle v_y \rangle}{\partial t} = \frac{\partial \mathrm{Re}_\phi}{\partial x} + \nu \frac{\partial^2 \langle v_y \rangle}{\partial x^2} \qquad (5)$$

From (5) one may see that in this case the Reynolds stress is a dynamo for the poloidal flow, since the poloidal flow is generated by the radial variance of the Reynolds stress and damped by the viscosity.

It is now interesting to compare the instant $\frac{\partial \mathrm{Re}_\phi}{\partial x} + \nu \frac{\partial^2 \langle v_y \rangle}{\partial x^2}$ value and the acceleration of the mean poloidal flow $\frac{\partial \langle v_y \rangle}{\partial t}$, since it correspond to the situation where a Reynolds stress has been measured and one wants to predict changes in the flow. The results are shown for four different times in Figures 3 and 4 for the Reynolds stress and the pseudo-Reynolds stress respectively. The $\frac{\partial \langle v_y \rangle}{\partial t}$ has been calculated as a simple difference. It is seen that for the real Reynolds stress case the correspondence is quite good (the deviations is due to the limited resolution of the radial derivative), and it is thus numerically demonstrated that the Reynolds stress acts as a dynamo for the poloidal flow. For the case of the pseudo-Reynolds stress calculated for the drift modes the correspondence is poorer for times $t > 100$. The reason is probably insufficient resolution of the density, which is cascaded to smaller scales. This causes the error in ∂_x to grow. Higher resolution simulations are presently being performed.

The validity of the results presented above are naturally limited by the assumptions of the relatively simple Hasegawa-Wakatani model. Furthermore, the approximation of the pseudo-Reynolds stress is a very rough method. However, the first-principles results indicate that the concept of performing accurate measurements of density fluctuations in order to predict the generation of shear flows may prove interesting.
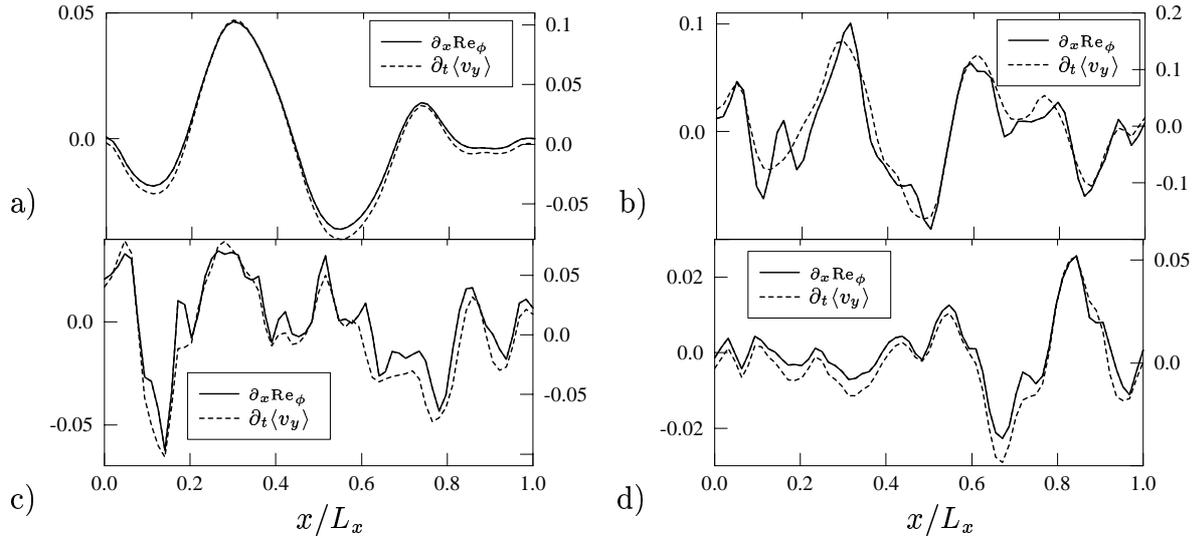
$\tilde{\phi}$

Figure 3: *The acceleration of the mean poloidal flow,* $\frac{\partial \langle v_y \rangle}{\partial t}$, *compared to the right hand side of (5),* $\frac{\partial Re_\phi}{\partial x} + \nu \frac{\partial^2 \langle v_y \rangle}{\partial x^2}$, *at times a) $t = 75$, b) $t = 100$, c) $t = 150$ and d) $t = 200$.*
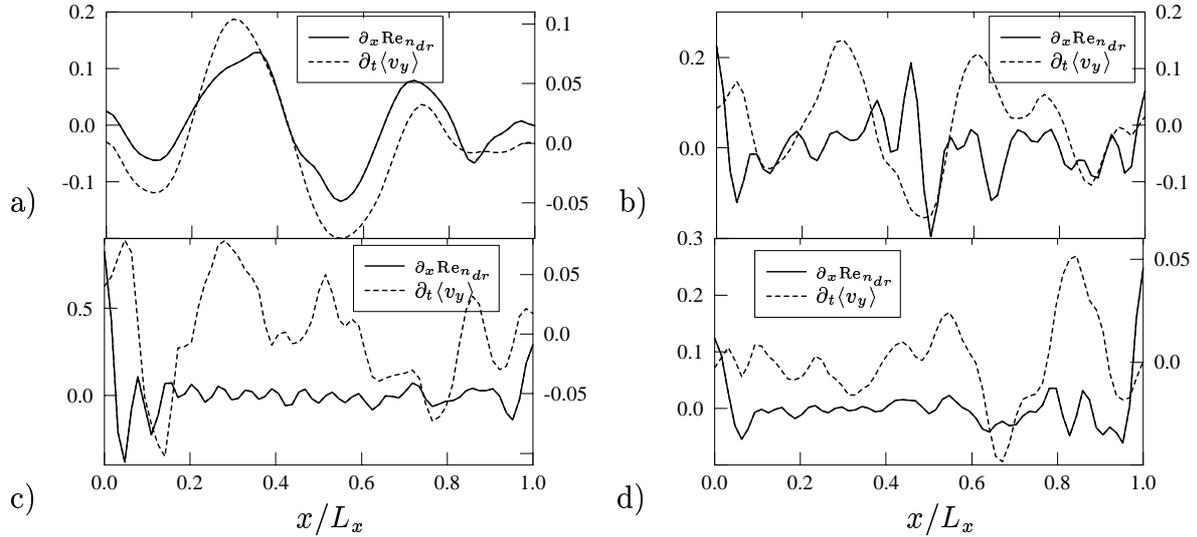

Figure 4: *The acceleration of the mean poloidal flow,* $\frac{\partial \langle v_y \rangle}{\partial t}$, *compared to* $\frac{\partial Re_{n_{drift}}}{\partial x} + \nu \frac{\partial^2 \langle v_y \rangle}{\partial x^2}$, *at times a) $t = 75$, b) $t = 100$, c) $t = 150$ and d) $t = 200$.*

References

[1] P. H. Diamond and Y.-B. Kim, Phys. Fluids B **3** (1991) 1626–1633.

[2] C. Hidalgo, C. Silva, M. A. Pedrosa, E. Sánchez, H. Fernandes, and C. A. F. Varandas, Phys. Rev. Lett. **83** (1999) 2203–2205.

[3] A. Hasegawa and M. Wakatani, Phys. Rev. Lett. **50** (1983) 682–686.

[4] S. B. Korsholm, P. K. Michelsen, and V. Naulin, Phys. Plasmas **6** (1999) 2401–2408.

[5] D. J. Triton, *Physical Fluid Dynamics*, Clarendon Press, Oxford, 2nd edition, 1988.

[6] V. Naulin, Europhys. Lett. **43** (1998) 533 – 538.

[7] B. LeBlanc, R. Bell, S. Bernabei, J. Hosea, R. Majeski, M. Ono, C. Phillips, J. Rogers, G. Shilling, C. Skinner, and J. Wilson, Phys. Rev. Lett. **82**(2) (1999) 331–334.